



## Study on the adsorption mechanism of activated carbon removing low concentrations of heavy metals

Lihua Dong<sup>a,b,c</sup>, Wenjun Liu<sup>b,\*</sup>, Renfu Jiang<sup>d</sup>, Zhansheng Wang<sup>b</sup>

<sup>a</sup>School of Environment, Tianjin University, Tianjin 300072, China, Tel. +86 01062796958; email: 1611415988@qq.com (L. Dong)

<sup>b</sup>School of Environment, Tsinghua University, Beijing 100084, China, email: wjliu@tsinghua.edu.cn (W. Liu),

zswang@tsinghua.edu.cn (Z. Wang)

<sup>c</sup>Department of Environmental Protection, Beijing Industrial Design and Research Institute, Beijing 100021, China

<sup>d</sup>Department of research and development, Taixing-Yixin Activated Carbon Co., Ltd., Taixing 225452, Jiangsu Province, China, Tel. +86 13852889397; email: 2787199785@qq.com

Received 6 November 2014; Accepted 20 September 2015

### ABSTRACT

This paper focused on the adsorption mechanism of activated carbon for the removal of low-concentration heavy metals in drinking water treatment. Two commercial activated carbon AC-1 and AC-2 were selected, which mainly were used for the terminal purification of drinking water. To investigate the differences of adsorption capacity of ACs for Pb, Hg, and As, scanning electron microscopy test (SEM), N<sub>2</sub> adsorption/desorption isotherm, the surface functional groups (FT-IR), the point zero charge (PZC), and X-ray photoelectron spectroscopy analysis were conducted. Freundlich isotherms were used to describe the adsorption behavior of ACs on heavy metal ions. The results showed that both AC-1 and AC-2 have aptitude for low-concentration heavy metals retention; taking the removal capacity and cost into account, AC-1 is more efficient and economic than AC-2 for the low-concentration heavy metal ions (Pb and Hg) removal from water. The mechanism analysis showed that the adsorption of ACs on low-concentration heavy metals heavily depends on the properties of ACs (pore size distribution, pH<sub>PZC</sub>, surface functional groups etc.) and the experiment condition, which cannot only be explained by ion exchange, chemical adsorption, specific adsorption, and electrostatic effects.

*Keywords:* Activated carbons; Heavy metals; Adsorption characteristics; Surface functional group; XPS analysis; Point of zero charge

### 1. Introduction

Heavy metals are nowadays among the most important pollutants in surface and groundwater, such

as lead, mercury, arsenic, cadmium, chromium, copper, and nickel, which have received considerable attention worldwide because of their toxicity on metabolism and intelligence [1]. Excessive ingestion of them can cause accumulative poisoning, cancer, nervous system damage, etc. [2,3]. Therefore, the

\*Corresponding author.

Presented at the 7th International Conference on Challenges in Environmental Science and Engineering (CESE 2014) 12–16 October 2014, Johor Bahru, Malaysia

elimination of heavy metals from water is important to protect public health. A number of treatment methods for removing metal ions from aqueous solutions have been well documented [4], which included oxidation, reduction, precipitation, membrane filtration, ion exchange, and adsorption. Among all the methods, adsorption is highly effective and economical because of its simplicity, convenience, and renewability. Several adsorbents have been studied for adsorption of metal ions such as activated carbon [5,6], multiwalled carbon nanotubes [7], fly ash [8,9], peat [10], sewage sludge ash [11], zeolite [12–14], kaolinite [15], and resins [16]. However, there is a requirement to remove the final traces of metal species during drinking water treatment. The European Community Directive 98/83 and the WHO guidelines set lead's value for tap waters at 10 µg/L from December 2013 [17]. China standards for drinking water quality, the maximum acceptable concentration for Pb, Hg, and As are, respectively, 10, 1, and 10 µg/L [18]. In this case, the common methods for removing heavy metals are either economically unfavorable (e.g. precipitation, conventional ion exchange, electrolyte or liquid extraction) or technically complicated (electrodialysis, reverse osmosis) [19–21]. At very low concentrations, such pollutants can be removed by adsorption on activated carbon [22], which has a high surface area, porous structure, and functional group and has been the most popular and widely used adsorbent in water treatment technology all over the world [23–26].

However, many studies for the removal of heavy metals were conducted under a higher concentration (5–700 mg/L) [27], there is little information on the analysis of adsorption mechanism of different ACs on heavy metals at low concentration ( $\leq 0.05$  mg/L). The objective of this study was to research the adsorption mechanism of two types of commercial activated carbons: AC-1 (from American) and AC-2 (from Japan), which mainly were used for the terminal purification of drinking water. The experiments of adsorption isotherm have been performed to evaluate ACs' adsorption potential for heavy metals Pb, Hg, and As from aqueous solutions.  $N_2$  adsorption/desorption isotherm, the Fourier transform infrared radiation (FTIR), point zero of charge (PZC), and X-ray photoelectron spectroscopy analysis (XPS) were tested to investigate the adsorption mechanism of heavy metals on AC-1 and AC-2, which are significant in guiding the selection of adsorbents for the removal of low-concentration heavy metals in water treatment and facilitating understanding of the adsorption mechanism.

## 2. Materials and methods

### 2.1. Samples description

Two types of commercial ACs used for the terminal purification of drinking water in drinking water: AC-1 and AC-2 were selected for the study. Considering the price, AC-2 (about 8 \$/kg) is two times that of AC-1 (about 4 \$/kg). AC-1 (purchased from American) was made from conventional activated carbon by modification, which was achieved by imparting the activated carbon ion-exchange properties. AC-2 (purchased from Japan) was a kind of AC filters used in drinking water treatment for the removal of heavy metals, which was a combination of 70–85% activated carbon and 15–30% of some filter, of which the filters are the main components for the removal of heavy metals and have a higher price (about 25 \$/kg).

### 2.2. Samples characterization

To investigate the surface micromorphology of materials, scanning electron microscopy (SEM) was performed using a FEI Quanta 200 SEM. The BET surface area and porous properties of AC-1 and AC-2 were obtained from  $N_2$  adsorption/desorption isotherms at 77 K using volumetric adsorption analyzer (Autosorb-iQ2-MP, Quantachrome). The micropore size distribution was based on density functional theory (DFT) using the software supplied by Quantachrome [26]. The mesopore size distributions were derived from desorption branch of the isotherm by using the Barrett-Joyner-Halenda (BJH) model based on the nitrogen adsorption data. The surface functional groups of the ACs were detected using a FTIR spectrometer (Fourier-870 FT-IR, America), where the spectra were recorded from 400 to 4,000  $cm^{-1}$ . XPS was conducted to examine the elemental composition and their chemical oxidation state near the carbon surface. The measurements were performed by a spectrometer (ESCALAB 250 Xi) with monochromatic AlK $\alpha$  and Mg/Al dual anode sources as X-ray source. All binding energies were referenced to the C 1s peak at 284.6 eV to compensate for the surface charging effects.

### 2.3. PZC measurements

Batch equilibrium method for the determination of PZC was proposed [28,29]. To quantify the PZC, 75 mg of AC was added to 50-mL conical flasks. A standard solution of a volume of 10 mL of 0.1 M NaCl

was added into each flask, whose initial pH had been adjusted with NaOH or HCl. The containers were sealed and placed on a shaker for 24 h and the resultant pH was recorded using a Mettler-Toledo 340 pH meter. Zeta potential measurements were conducted on a DelsaNano C (Beckman Coulter Co., Ltd) immediately after the pH measurements of the samples. The measurements were measured three times for a single sample to provide an average reading. Between the samples, the cell was flushed with 30 ml of ultrapure water. The PZC occurs when there is no change in the pH after contact with the carbon.

#### 2.4. Adsorption experiments

Adsorptive capacities of activated carbon were determined according to ASTM standards (second edition, 2000). AC-1 and AC-2 were reduced in particle size so that 95% passes through a US 325-mesh sieve. All reagents used were of analytical reagent grade. All glassware were pretreated with nitric acid overnight. Desired concentration of solutions, Pb (50 µg/L), Hg (15 µg/L), and As (50 µg/L), were obtained by diluting the standard solution of heavy metal (1,000 µg/mL, Iron and Steel Institute ng Detection Technology Co. Ltd) in ultrapure water provided by a Milli-Q from Millipore Corporation, USA. Measure 500 ml aliquots into 1,000 ml glass-stoppered Erlenmeyer flask and then, add appropriate amount of pulverized AC to the containers. Adsorption experiments were conducted in a water bath shaker at 120 rpm and the desired temperature (25°C). After 2 h, the samples were immediately filtered through 0.45-µm polyethersulfone membrane filters to remove the activated carbon and the concentrations of Pb, As in solution were determined with an ICP-MS (XSeries<sup>II</sup>, Thermo Electron Corporation, USA), the concentrations of Hg are measured using AFS220 + SA-10/20 (Beijing Titan Instruments, China). In all the experiments, blanks of the metal were made. Recoveries were determined in triplicates and the average values are reported.

#### 2.5. Data analysis

Two widely used isotherm models, Freundlich and Langmuir were examined to fit the experimental data. The results indicated that the Freundlich model produced good fits. Therefore, the Freundlich model was selected for data analysis in this study:

$$q_e = (C_0 - C_e)V/M = KC_e^{1/n} \quad (1)$$

where  $q_e$  is the amount of heavy metal adsorbed, µg/mg;  $C_0$  and  $C_e$  are the initial and equilibrium concentrations of the heavy metal in solution, µg/L;  $V$  is the volume of solution, L; and  $M$  is the mass of the adsorbent, mg;  $K$  and  $n$  are the constants of Freundlich isotherms, and  $K$  was used to represent the activated carbon adsorption capacities at equilibrated concentrations of 1 µg/L [30].

### 3. Results and discussion

#### 3.1. Characterization of adsorbents

##### 3.1.1. Scanning electron microscopy

Because the adsorption experiments were conducted under the same bath temperature and stirring speed, the external mass transfer resistance is assumed to be absent. Adsorption of heavy metals is basically governed by intraparticle surface diffusion, where pore size distribution and surface characteristics are important. SEM micrograph (5,000× magnification) of AC-1 and AC-2 is shown in Fig. 1. AC-1 has an irregular morphology formed by the aggregates of different size particles, where the fibrous nature of the structure is not so predominant. Different from AC-1, the surface structure of AC-2 shows porous structure containing more macropores in it, especially the cavernous pores of about 20-µm diameter, which may be an inherent fiber structure in the original raw material of AC-2. It can be seen that the pores in AC-2 are not interconnected, which may not favor the diffusion of the heavy metal ion into the inner surface of AC-2.

##### 3.1.2. $S_{BET}$ and porosity characteristics of ACs

The adsorption properties of AC depend not only on its surface properties, but also on its pore structure. To examine the specific surface area and porosity characteristics of ACs, nitrogen adsorption/desorption experiments at 77 K were performed using an auto-sorb apparatus which is shown in Fig. 2.

Fig. 2 indicates that the adsorption/desorption isotherm types for AC-1 and AC-2 have obvious differences. The isotherm for AC-2 clearly belongs to type I with a slight hysteresis loop, which indicated the pore structure in AC-2 was dominated by micropores. However, for AC-1, the isotherm is clearly a mixture of types I and II and has a significant hysteresis loop, which revealed the existence of micropores, mesopores, and macropores simultaneously [31].

According to the international union of pure and applied chemistry (IUPAC) classification of adsorption isotherms, the pores of AC include three groups:

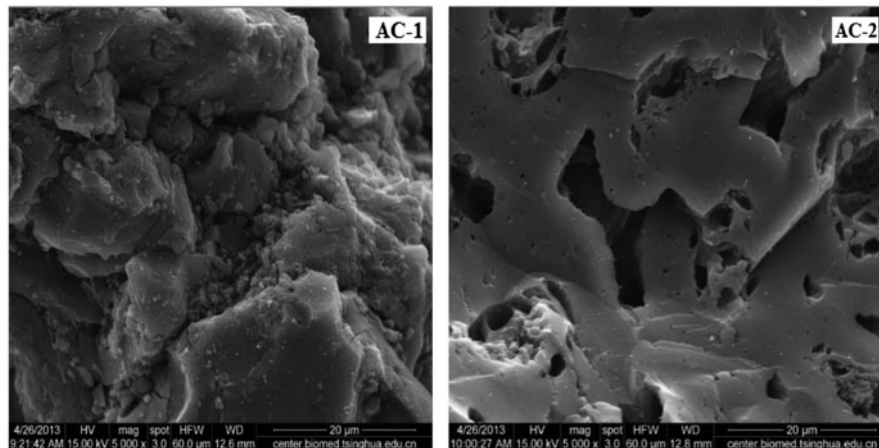


Fig. 1. SEM micrograph of AC-1 and AC-2.

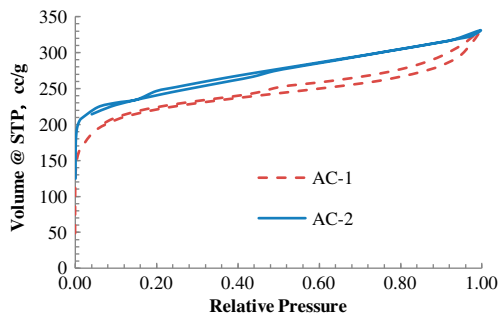


Fig. 2. Adsorption/desorption isotherms of  $N_2$  at 77 K for AC-1 and AC-2.

macropore width (>50 nm), mesopore width (2–50 nm), and micropore width (<2 nm). Porous structure parameters of AC-1 and AC-2 are listed in Table 1. As Table 1 indicates  $S_{BET}$ ,  $D_{av}$ , and  $V_{mic}/V_{total}$  of AC-1 and AC-2 are very similar. The difference is that  $V_{meso}/V_{total}$  for AC-1 is three times of AC-2, namely the majority of pores for AC-2 fall into the range of micropores and macropores, but AC-1 has a large proportion of mesopores in it.

### 3.1.3. FT-IR analysis

The adsorption properties of activated carbon depend not only on its pore structure, but also on its surface chemical properties. The type and quantity of activated carbon surface functional groups can significantly affect the behavior of activated carbon [32]. FTIR was performed using a Fourier-870 FT-IR (America). KBr powder was used as the background.

FTIR spectra are shown in Fig. 3, a broad band between 3,100 and 3,700  $cm^{-1}$  for AC-1 and AC-2 indicates the presence of both free and hydrogen-bonded OH groups on the adsorbent surface [33]. This stretching is due to the adsorbed water (peak at 3,400  $cm^{-1}$ ) on the surface [34]. The FTIR spectra of AC-2 indicated broad peaks in the region of 1,600–1,800  $cm^{-1}$  corresponding to CO group stretching from aldehydes and ketones; among them, a maximum peak at 1,640  $cm^{-1}$  can be assigned to the C=C stretching vibration in polynuclear aromatic compounds in the sample [35,36]. For AC-1, the peak at 1,100  $cm^{-1}$  is due to –C–O–H stretching and –OH deformation values. The presence of polar groups on the surface is likely to give considerable cation-exchange capacity [37].

Table 1  
Porous structure parameters of AC-1 and AC-2

Name	$S_{BET}$ ( $m^2/g$ )	$S_{mic}$ ( $m^2/g$ )	$D_{av}$ (nm)	$V_{total}$ ( $cm^3/g$ )	$V_{mic}$ ( $cm^3/g$ )	$V_{mic}/V_{total}$ (%)	$V_{meso}$ ( $cm^3/g$ )	$V_{meso}/V_{total}$ (%)
AC-1	739.7	621.4	2.752	0.5089	0.2997	58.89	0.1292	25.4
AC-2	777.4	579.5	2.635	0.5121	0.3013	58.84	0.0422	8.24

Notes:  $S_{BET}$ : BET specific surface area;  $S_{mic}$ : micropore volume;  $D_{av}$ : average pore diameter;  $V_{total}$ : total pore volume and  $V_{meso}$ : mesopore volume.

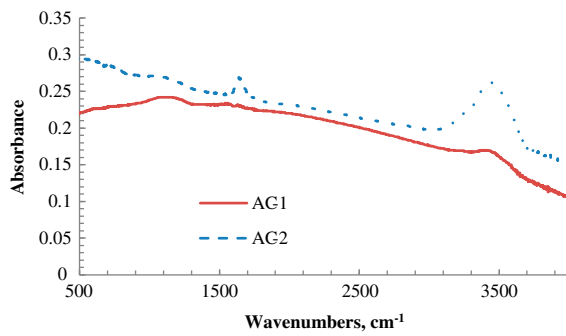


Fig. 3. FTIR spectrums of AC-1 and AC-2.

### 3.2. Adsorption of heavy metals on AC-1 and AC-2

Because AC-1 and AC-2 are used for terminals purification of drinking water, the adsorption experiments of AC-1 and AC-2 were conducted under a neutral pH range (6–8) and low-level concentration, which are closer to the actual application conditions. Combined with the standards for drinking water quality of China, the initial concentrations for Pb, Hg, and As solution are, respectively, set at 50, 15, and 50  $\mu\text{g/L}$ .

#### 3.2.1. Pb adsorption

Fig. 4a shows the adsorption character of AC-1 can be well fitted by Freundlich adsorption isotherm ( $R^2 = 0.986$ ,  $K = 0.0018$ ), but the adsorption of AC-2 for Pb ion has a bad fit and did not exhibit any regularity.

The effect of adsorbent dosage on Pb ion removal percentage and adsorption capacity of ACs is given in Fig. 4b, which indicated AC-1 has a good removal effect for heavy metal Pb at low concentrations and low carbon-dosing and AC-2 has a poor adsorption

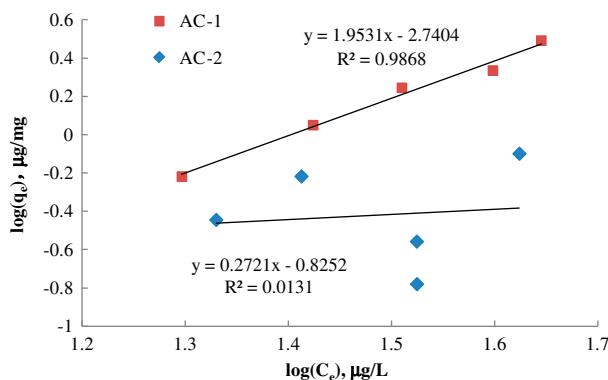


Fig. 4a. Freundlich adsorption isotherm of Pb on AC-1 and AC-2. (pH 7.0, equilibrium time = 2 h, temperature = 25 °C).

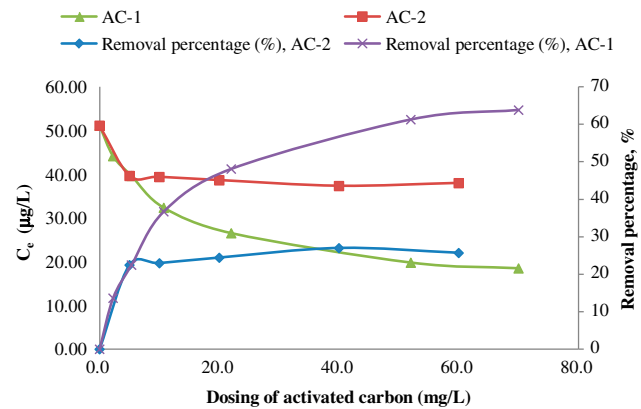


Fig. 4b. Dosage effects on the adsorption capacity of Pb for AC-1 and AC-2. (pH 7.0, equilibrium time = 2 h, temperature = 25 °C).

effect. It can be seen from Fig. 4b that the Pb ion removal percentages of AC-1 and AC-2 increase sharply to, respectively, 36.7 and 23% with the increase in the ACs dose from 0 to 10 mg. With further increase in the adsorbent dosage from 10 to 60 mg, the Pb ion removal percentage of AC-1 gradually increases to 62%, but for AC-2, the Pb ion removal percentage did not change with the increase in the adsorbent dosage. This may be due to the greater adsorbent surface area ( $S_{\text{BET}}$ , 777.4  $\text{m}^2/\text{g}$ ) and micropore volume ( $V_{\text{micr}}$ , 0.3013  $\text{m}^3/\text{g}$ ) available in AC-2 providing more functional groups and active adsorption sites that result in a higher Pb ion initial removal percentage [27]. As mentioned above, the adsorption of heavy metals is basically governed by intraparticle surface diffusion in the experiment. Compared with AC-2, besides a relatively higher specific surface area ( $S_{\text{BET}}$ , 739.7  $\text{m}^2/\text{g}$ ) and micropore volume ( $V_{\text{micr}}$ , 0.2997  $\text{m}^3/\text{g}$ ), AC-1 also has a greater  $V_{\text{meso}}/V_{\text{total}}$ . The higher mesopore volume in AC-1 ( $V_{\text{meso}}$ , 0.1292  $\text{m}^3/\text{g}$ ) can serve as the transport pathway, which is conducive to the intraparticle surface diffusion, therefore, AC-1 can fully use all active sites, leading to a higher adsorption capacity; as for AC-2 ( $V_{\text{meso}}$ , 0.0422  $\text{m}^3/\text{g}$ ) with fewer transport pathway, only a part of active sites are occupied by Pb ions, leading to a lower adsorption capacity [38]. SEM micrograph of AC-1 and AC-2 also confirmed the results. It was concluded that initially, the metals were absorbed by the active sites on the ACs surface and then diffused into the interior pores of the ACs.

#### 3.2.2. Hg adsorption

Freundlich adsorption isotherms of AC-1 and AC-2 for Hg are listed in Fig. 5a. Seen from Fig. 5a,  $R^2$

values of AC-1 and AC-2 are, respectively, 0.977 and 0.734, namely compared with AC-2, AC-1 can be well fitted by Freundlich adsorption isotherms. In addition, AC-1 has a larger  $K$  value ( $2.46 \times 10^{-2}$ ) than AC-2 ( $1.38 \times 10^{-4}$ ), which indicated that AC-1 has better adsorption effect than AC-2 for the heavy metal Hg at low concentration.

Fig. 5b clearly shows the effect of adsorbent dosage on Hg ion removal percentage and adsorption capacity of ACs, which has the similar shape with AC-1, namely with the increase in the adsorbent dose from 0 to 10 mg, both AC-1 and AC-2 have a higher initial removal percentage. With further increase in adsorbent dosage, the removal percentages of AC-1 have an obvious increase and AC-2 is slowly increasing, and finally both AC-1 and AC-2 entered a platform phase, which can be attributed to the same cause with the adsorption of Pb. In summary, the removal percentage of AC-1 (>80%) is far above AC-2 (56%) in the same experiment condition, namely considering the removal capacity of material, AC-1 is more efficient than AC-2 for Hg adsorption.

### 3.2.3. As adsorption

For As, AC-1 has a slight adsorption effect, the maximum removal percentage was only 8.3% and AC-2 has no removal, which may be due to the anionic form of arsenic in the solution, leading to electrostatic repulsion.

Overall, both AC-1 and AC-2 have aptitude for low-concentration heavy metals retention; taking the removal capacity into account, AC-1 is more efficient than AC-2 for Pb, Hg, and As adsorption at the same experiment conditions.

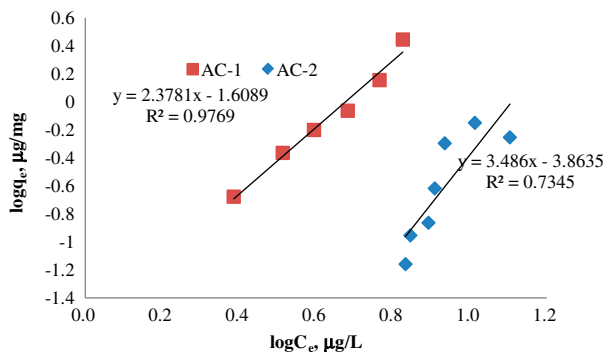


Fig. 5a. Freundlich adsorption isotherm of Hg on AC-1 and AC-2. (pH 7.0, equilibrium time = 2 h, temperature = 25 °C).

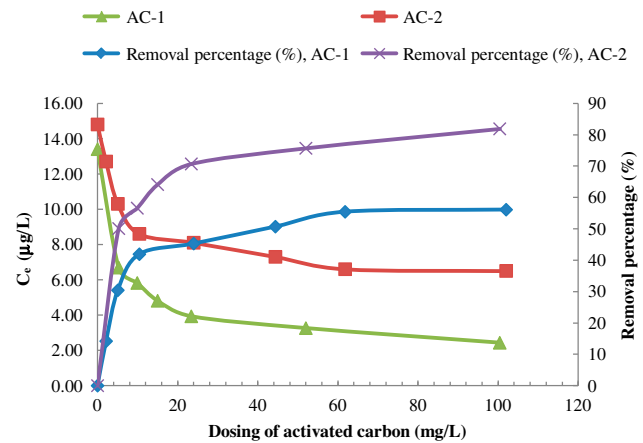


Fig. 5b. Dosage effects on the adsorption capacity of Hg for AC-1 and AC-2. (pH 7.0, equilibrium time = 2 h, temperature = 25 °C).

### 3.2.4. Comparison of cost and the adsorption capacity of AC-1 and AC-2

The removal of heavy metals by activated carbons has been widely reported, in which the heavy metal concentration was usually in a higher level (5–700 mg/L). Li et al. [27] gave a survey of adsorption capacities of Pb(II) ions by various adsorbents, of which EPAC has the largest adsorption capacity of 146.85 mg/g with a 60 mg/L initial Pb ion concentration and a carbon dosage of 0.5 g/L. Hassan et al. [39] listed the adsorption capacities for some adsorbents used for mercury(II) removal from water and Rao et al. [40] compared the adsorption capacity of different activated carbons for Hg(II), in which the activated carbon from furfural has the largest adsorption capacity of 174 mg/g, with a 40 mg/L initial Hg ion concentration, and a carbon dosage of 200 mg/L [41], which is larger than that of the antibiotic-activated carbon (129 mg/g) [42], the granular activated carbon (0.8 mg/g) [43], PHC-peanut carbon (110 mg/g) [44], and coir pith-activated carbon (154 mg/g) [45]. Of which only the literature [43] was about drinking water treatment, others were for high-concentration heavy metals removal, also, most of them did not give the information of cost. Therefore, the comparison of cost and adsorption capacity was only conducted for AC-1 and AC-2 (see Table 2).

It can be seen from Table 2 that both AC-1 and AC-2 have aptitude for low-concentration heavy metals retention; taking the removal capacity and cost into account, AC-1 is more efficient and economic than AC-2 for the low-concentration heavy metal ions (Pb and Hg) removal from drinking water.

Table 2

Comparison of the efficiency and cost of AC-1 and AC-2 for low-concentration heavy metals

Name	Cost (\$/kg)	Pb		Hg	
		Adsorption capacity (mg/g)	Removal (%)	Adsorption capacity (mg/g)	Removal (%)
AC-1	4	3.1	63.8	2.78	81.87
AC-2	8	0.49	25.7	1.0	53.24

### 3.3. Adsorption mechanisms analysis

#### 3.3.1. PZC analysis

PZC is defined as the pH at which carbon surface has no charge, namely the zeta ( $\zeta$ ) potential is zero. The zeta ( $\zeta$ ) potential variations of AC-1 and AC-2 were estimated considering the pH of solution on a DelsaNano C (Beckman Coulter Co., Ltd) and this variation is given in Fig. 6.

From Fig. 6, it can be seen that the zeta potentials of AC-1 and AC-2 increase in the negative direction with the increase in the pH of solution due to the ionization of acidic oxygen surface groups. The PZCs of AC-1 and AC-2 are, respectively, 5.7 and 7.2, namely the carbon surface is negatively charged at pH values above  $\text{pH}_{\text{PZC}}$  ( $\text{pH} > 5.7$  for AC-1 and  $\text{pH} > 7.2$  for AC-2) and positively charged at pH values below  $\text{pH}_{\text{PZC}}$  [46].

During the experiments (conducted at pH 7), the AC-1 surface is negatively charged, which can promote the adsorption of the positively charged metal ions from solution due to the electrostatic attractive interactions between them. In addition, the negative surface charge is also conducive to ionization of the ion-exchange functional groups in AC-1 (Fig. 3). As for AC-2, the surface is positively charged, which will repel cations due to the electrostatic force of repulsion. FT-IR spectrum (Fig. 3) indicated that there was a higher absorbance peak of hydrogen-bonded OH groups on the surface of AC-2, which should contribute to the initial adsorption of heavy metal ion. However, the competition of  $\text{H}^+$  and heavy ions for the same adsorption active sites leads to lower heavy

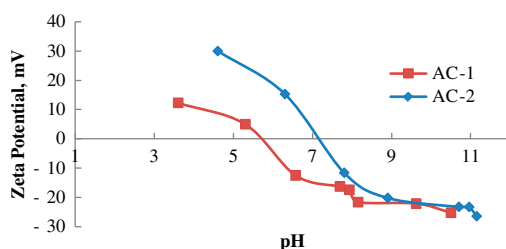


Fig. 6. Zeta potentials at different pH values.

metal ion adsorption capacity of AC-2. As far as electrostatic effects are considered, AC-2 should have a good removal for the arsenic, but the result is contrary, which indicates not only electrostatic effects and chemical adsorption but also plays an important role.

The analysis indicated that the pH of the solution is one of the most important factors to determine the adsorption property of an adsorbent due to its effect on the surface charge of adsorbent and ionization of adsorbent.

#### 3.3.2. Analysis of elemental composition before and after adsorption

XPS measurements were carried out in order to fully investigate the adsorption mechanisms of AC-1 and AC-2 on low-concentration heavy metals. The atomic compositions, summarized in Table 3, which showed both AC-1 and AC-2, are composed mainly of carbon and oxygen before adsorption. The O/C ratio in AC-1 (11.2%) is higher than that in the AC-2 sample (8.48%), namely AC-1 contains more oxygen functional groups before adsorption.

From Table 3, it was also found that the oxygen contents of AC-1 and AC-2 after adsorption were significantly increased, whereas the carbon content decreased. These results explicitly show the forming (or introducing) of surface oxygen complexes as a result of the adsorption.

XPS spectrum (Fig. 7) indicated that Pb and Hg were detected on the surface of AC-1 after adsorption, in which Pb 4f showed a broad and weak peak from 147.83 to 134.53 eV, Hg 4f spectra exhibited intensive peaks at 103.47 eV (Fig. 7). In the case of AC-2, Hg 4f spectra were observed at 103.98 eV and Pb was below detective limits, namely both AC-1 and AC-2 have aptitude for heavy metal retention, which confirmed the results of experiment.

#### 3.3.3. Analysis of surface functional groups before and after adsorption

To facilitate the understanding of adsorption mechanism, the O 1s peaks before and after adsorption are

Table 3  
Elemental composition of AC-1 and AC-2 before and after Pb, Hg adsorption

Name	C 1s, Atomic (%)	O 1s, Atomic (%)	Hg 4f, Atomic (%)	Pb 4f, Atomic (%)	O/C Ratio (%)
AC-1	89.97	10.03	–	–	11.2
AC-2	92.18	7.82	–	–	8.48
After Pb adsorption (AC-1)	88.15	11.83	0.01	0.01	13.4
After Hg adsorption (AC-1)	88.53	11.44	0.03	–	0.129
After Pb adsorption (AC-2)	91.26	8.72	0.02	–	9.56
After Hg adsorption (AC-2)	90.99	8.99	0.03	–	9.88

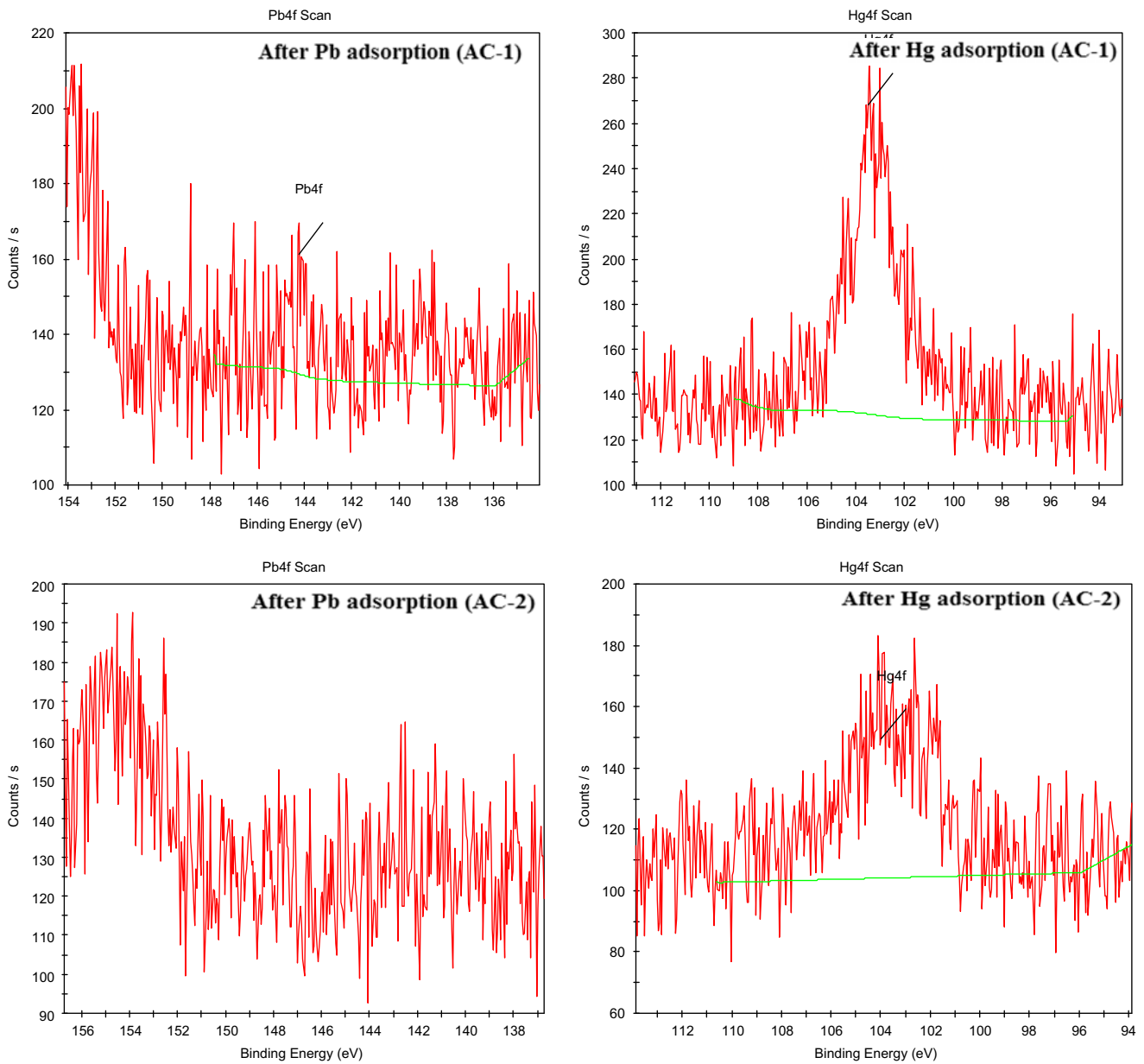


Fig. 7. XPS spectra of Pb 4f and Hg 4f for AC-1 and AC-2 before and after adsorption.

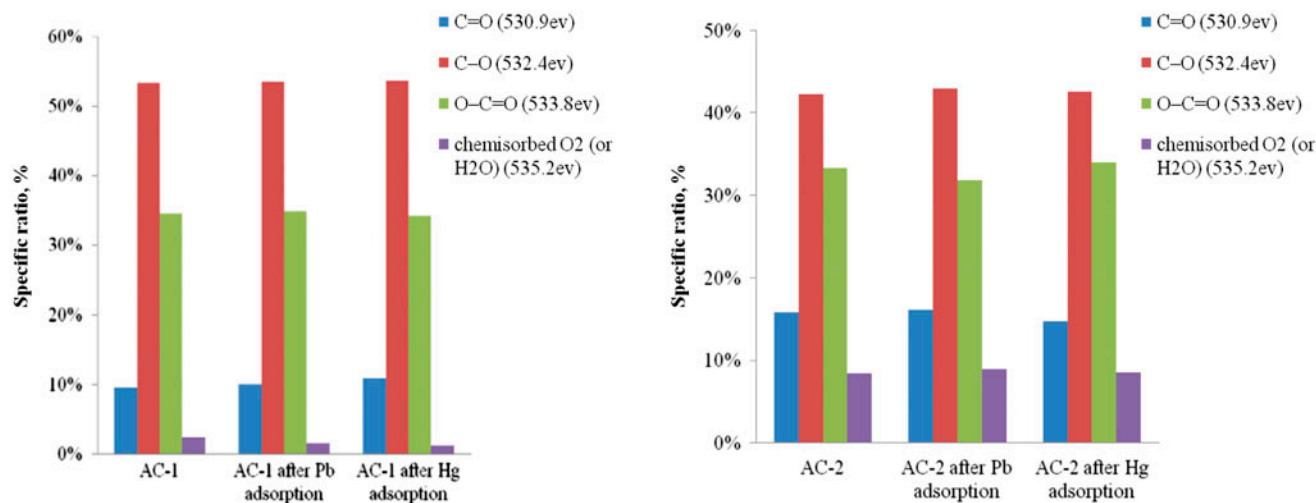


Fig. 8. Specific ratios of surface functional groups of AC-1 and AC-2 in the O 1s-XPS results.

deconvoluted into surface oxygen complex contributions [47] and the specific ratios of the contributions are also provided, which are given in Fig. 8. As can be observed in the deconvoluted O 1s spectra, the main component located at 532.4 eV (53.5% peak area for AC-1 and 42.3% for AC-2) is related to C–O (H). The high-energy subpeak centered at 533.8 eV (34.6% peak area for AC-1 and 33.4% for AC-2) corresponds to carboxyl groups (H) O–C=O. Comparison of the two spectra shows that the higher oxygen concentration found for AC-1 is related to a higher quantity of C–O (H) and (H) O–C=O groups in this sample, observed as an intensity increase of these components. These results are consistent with FT-IR, which should be responsible for the higher retention capacity of AC-1 [48].

Fig. 8 clearly shows the changes of functional groups after the adsorption. As for AC-1, it was found that the ratios of C=O increased whereas that of chemisorbed O<sub>2</sub> (or H<sub>2</sub>O) decreased after Pb and Hg adsorption; the ratios of C–O (H), (H) O–C=O did not change significantly, namely that the combination of heavy metal and chemisorbed O<sub>2</sub> (or H<sub>2</sub>O) leads to a decrease in the ratio of chemisorbed O<sub>2</sub> (or H<sub>2</sub>O) and an increase in C=O, which indicates chemical adsorption and electrostatic interactions play a dominant role in the adsorption of AC-1 on Pb and Hg. In the case of AC-2, the ratios of C=O significantly decreased whereas that of C–O (H), (H) O–C=O, and chemisorbed O<sub>2</sub> (or H<sub>2</sub>O) almost have no change after Hg adsorption, which should be due to the positive surface charge forcing heavy metal ions away from the positively charged C–O (H) and (H) O–C=O, near the uncharged C=O, namely the hydroxyl C–O (H) and

carboxyl groups (H) O–C=O didn't play a role in the ion exchange for the adsorption of AC-2 on Hg. The results indicate that the adsorption mechanism of AC-2 on Hg should be attributed to specific adsorption and electrostatic effects, which is completely different from AC-1. In summary, the adsorption mechanism of ACs on heavy metal ions cannot only be explained by ion exchange, chemical adsorption, specific adsorption, and electrostatic effects, which heavily depend on the experiment conditions and the properties of ACs.

#### 4. Conclusions

This paper studied the adsorption mechanism of two kinds of ACs for the removal of low-concentration heavy metals Pb, Hg, and As in drinking water treatment. The results showed that both AC-1 and AC-2 have aptitude for low-concentration heavy metals retention from water; taking the removal capacity and the cost into account, AC-1 is more efficient than AC-2.

The adsorption mechanism analysis indicated the adsorption of ACs on low-concentration heavy metals was basically governed by the properties of ACs and the experiment condition. The metals were initially absorbed by the active sites on the ACs surface, and then diffused into the interior pores of the ACs, where pore size distribution and surface characteristics played an important role, which basically governed the adsorption of heavy metals by intraparticle surface diffusion, namely the adsorption mechanism of ACs on low-concentration heavy metals heavily depends on the properties of ACs (pore size distribution,

pH<sub>PZC</sub>, surface functional groups etc.) and the experiment condition, which cannot only be explained by ion exchange, chemical adsorption, specific adsorption, and electrostatic effects. The results are significant in guiding the selection of AC for the removal of low-concentration heavy metals and facilitating understanding of the adsorption mechanism.

### Acknowledgements

The work has been supported by the National Water Special Project for the 12th five-year plan (No. 2011ZX07415-00) and the National Water Special Project (No. 2012ZX07404002).

### References

- [1] S. Taha, S. Ricordel, I. Cisse, Kinetic study and modeling of heavy metals removal by adsorption onto peanut husks incinerated residues, *Energy Procedia* 6 (2011) 143–152.
- [2] L. Friberg, G.F. Nordberg, B. Vouk, *Handbook on the Toxicology of Metals*, Elsevier, Amsterdam, 1979.
- [3] J. Calderón, M.E. Navarro, M.E. Jimenez-Capdeville, M.A. Santos-Diaz, A. Golden, I. Rodriguez-Leyva, V. Borja-Aburto, F. Díaz-Barriga, Exposure to arsenic and lead and neuropsychological development in Mexican children, *Environ. Res.* 85 (2001) 69–76.
- [4] J.W. Patterson, *Industrial Wastewater Treatment Technology*, second ed., Butterworth-Heinemann, London, 1985.
- [5] M.M. Rao, A. Ramesh, G.P.C. Rao, K. Seshiah, Removal of copper and cadmium from the aqueous solutions by activated carbon derived from ceiba pentandra hulls, *J. Hazard. Mater.* 129 (2006) 123–129.
- [6] M. Sekar, V. Sakthi, S. Rengaraj, Kinetics and equilibrium adsorption study of lead(II) onto activated carbon prepared from coconut shell, *J. Colloid Interface Sci.* 279 (2004) 307–313.
- [7] M.R. Lasheen, I.Y. El-Sherif, D.Y. Sabry, S.T. El-Wakeel, M.F. El-Shahat, Adsorption of heavy metals from aqueous solution by magnetite nanoparticles and magnetite-kaolinite nanocomposite: Equilibrium, isotherm and kinetic study, *Desalin. Water Treat.* 53 (2015) 1–10.
- [8] J. Hizal, E. Tutem, K. Guclu, M. Hugul, S. Ayhan, R. Apak, F. Kilinckale, Heavy metal removal from water by red mud and coal fly ash: An integrated adsorption-solidification/stabilization process, *Desalin. Water Treat.* 51 (2013) 7181–7193.
- [9] T.S. Malarvizhi, T. Santhi, Adsorption of Zn(II) ions from aqueous solution on lignite-fired fly ash, *Desalin. Water Treat.* 51 (2013) 6777–6788.
- [10] Y.S. Ho, G. McKay, The sorption of lead(II) ions on peat, *Water Res.* 33 (1999) 578–584.
- [11] S.C. Pan, C.C. Lin, D. Tseng, Reusing sewage sludge ash as adsorbent for copper removal from wastewater, *Resour. Conserv. Recycl.* 39 (2003) 79–90.
- [12] L.H. Kim, H.M. Kang, W. Bae, Treatment of particulates and metals from highway stormwater runoff using zeolite filtration, *Desalin. Water Treat.* 19 (2010) 97–104.
- [13] S. Wang, Y. Peng, Natural zeolites as effective adsorbents in water and wastewater treatment, *Chem. Eng. J.* 156 (2010) 11–24.
- [14] A. Mamdouh, A.A. Sameer, Use of Jordanian natural zeolite as sorbent for removal of cadmium from aqueous solutions, *Desalin. Water Treat.* 22 (2010) 349–354.
- [15] M. Arias, M.T. Barral, J.C. Mejuto, Enhancement of copper and cadmium adsorption on kaolin by the presence of humic acids, *Chemosphere* 48 (2002) 1081–1088.
- [16] C.V. Diniz, F.M. Doyle, V.S.T. Ciminelli, Effect of pH on the adsorption of selected heavy metal ions from concentrated chloride solutions by the chelating resin dowex M-4195, *Sep. Sci. Technol.* 37 (2002) 3169–3185.
- [17] R. Sublet, M.O. Simonnot, A. Boireau, M. Sardin, Selection of an adsorbent for lead removal from drinking water by a point-of-use treatment device, *Water Res.* 37 (2003) 4904–4912.
- [18] People's Republic of China National Standard, Standards for Drinking Water Quality, GB 5749-2006, Chinese Standards Press, Beijing, 2006.
- [19] J.W. Patterson, *Metals control technology: Past, present and future*, in: J.W. Patterson, R. Passino (Eds.), *Proceedings of the Second International Symposium on Metals Speciation, Separation and Recovery*, Lewis Publishers, Chelsea, Michigan, 1989, pp. 27–42.
- [20] J. Horacek, L. Soukupova, M. Puncochar, J. Slezak, J. Drahos, K. Yoshida, A. Tsutsumi, Purification of waste waters containing low concentrations of heavy metals, *J. Hazard. Mater.* 37 (1994) 69–76.
- [21] P. Brown, I.A. Atly Jefcoat, D. Parrish, S. Gill, E. Graham, Evaluation of the adsorptive capacity of peanut hull pellets for heavy metals in solution, *Adv. Environ. Res.* 4 (2000) 19–29.
- [22] B. Xiao, K.M. Thomas, Competitive adsorption of aqueous metal ions on an oxidized nanoporous activated carbon, *Langmuir* 20 (2004) 4566–4578.
- [23] E. Demirbas, M. Kobya, S. Öncel, S. Şencan, Removal of Ni(II) from aqueous solution by adsorption onto hazelnut shell activated carbon: Equilibrium studies, *Bioresour. Technol.* 84 (2002) 291–293.
- [24] T.M. Zewail, S.A.M. El-Garf, Preparation of agriculture residue based adsorbents for heavy metal removal, *Desalin. Water Treat.* 22 (2010) 363–370.
- [25] B. Thouraya, O. Abdelmottaleb, F. Nuria, V. Isabe, Single and binary adsorption of some heavy metal ions from aqueous solutions by activated carbon-derived from olive stones, *Desalin. Water Treat.* 53 (2015) 1082–1088.
- [26] A.S. Sartape, A.M. Mandhare, P.P. Salvi, D.K. Pawar, S.S. Kolekar, Kinetic and equilibrium studies of the adsorption of Cd(II) from aqueous solutions by wood apple shell activated carbon, *Desalin. Water Treat.* 51 (2013) 4638–4650.
- [27] Y.H. Li, Q.J. Du, X.D. Wang, P. Zhang, D.C. Wang, Z.H. Wang, Y.Z. Xia, Removal of lead from aqueous solution by activated carbon prepared from *Enteromorpha prolifera* by zinc chloride activation, *J. Hazard. Mater.* 183 (2010) 583–589.

- [28] P. Chingombe, B. Saha, R.J. Wakeman, Surface modification and characterisation of a coal-based activated carbon, *Carbon* 43 (2005) 3132–3143.
- [29] J.P. Reymond, F. Kolenda, Estimation of the point of zero charge of simple and mixed oxides by mass titration, *Powder Technol.* 103 (1999) 30–36.
- [30] M. El-Merraoui, M. Aoshima, K.K. Kaneko, Micropore size distribution of activated carbon fiber using the density functional theory and other methods, *Langmuir* 16 (2000) 4300–4304.
- [31] S.J. Zhang, T. Shao, H.S. Kose, T. Karanfil, Adsorption of aromatic compounds by carbonaceous adsorbents: A comparative study on granular activated carbon, activated carbon fiber, and carbon nanotubes, *Environ. Sci. Technol.* 44 (2010) 6377–6383.
- [32] G.G. Stavropoulos, A.A. Zabaniotou, Production and characterization of activated carbons from olive-seed waste residue, *Microporous Mesoporous Mater.* 82 (2005) 79–85.
- [33] L. Gu, D.D. Wang, R. Deng, H.X. Liu, H.N. Ai, Effect of surface modification of activated carbon on its adsorption capacity for bromate, *Desalin. Water Treat.* 51 (2013) 2592–2601.
- [34] M.M. Abou-Mesalam, Sorption kinetics of copper, zinc, cadmium and nickel ions on synthesized silico-antimonate ion exchanger, *Colloids Surf., A: Physicochem. Eng. Aspects* 225 (2003) 85–94.
- [35] M.P. Elizalde-González, J. Mattusch, A.A. Peláez-Cid, R. Wennrich, Characterization of adsorbent materials prepared from avocado kernel seeds: Natural, activated and carbonized forms, *J. Anal. Appl. Pyrolysis* 78 (2007) 185–193.
- [36] S.K. Sengupta, O.P. Pandey, A. Rai, A. Sinha, Synthesis, spectroscopic, thermal and antifungal studies on lanthanum(III) and praseodymium(III) derivatives of 1,1-diacetylferrocenyl hydrazones, *Spectrochim. Acta Part A: Mol. Biomol. Spectrosc.* 65 (2006) 139–142.
- [37] Y.S. Ho, C.C. Chiang, Y.C. Hsu, Sorption kinetics for dye removal from aqueous solution using activated clay, *Sep. Sci. Technol.* 36 (2001) 2473–2488.
- [38] V.K. Gupta, A. Rastogi, Biosorption of lead from aqueous solutions by green algae *Spirogyra* species: Kinetics and equilibrium studies, *J. Hazard. Mater.* 152 (2008) 407–414.
- [39] S.S.M. Hassan, N.S. Awwad, A.H.A. Aboterika, Removal of mercury(II) from wastewater using camel bone charcoal, *J. Hazard. Mater.* 154 (2008) 992–997.
- [40] M.M. Rao, D.H.K. Kumar Reddy, P. Venkateswarlu, K. Seshaiiah, Removal of mercury from aqueous solutions using activated carbon prepared from agricultural by-product/waste, *J. Environ. Manage.* 90 (2009) 634–643.
- [41] M.F. Yardim, T. Budinova, E. Ekinci, N. Petrov, M. Razvigorova, V. Minkova, Removal of mercury(II) from aqueous solution by activated carbon obtained from furfural, *Chemosphere* 52 (2003) 835–841.
- [42] T. Budinova, N. Petrov, J. Parra, V. Baloutzov, Use of an activated carbon from antibiotic waste for the removal of Hg(II) from aqueous solution, *J. Environ. Manage.* 88 (2008) 165–172.
- [43] X. Ma, K.S. Subramanian, C.L. Chakrabarthy, R. Goo, J. Cheng, Y. Lu, F.J. Pickering, Removal of trace mercury(II) from drinking water: Sorption by granular activated carbon, *J. Environ. Sci. Health A* 27 (1992) 1389–1396.
- [44] C. Namasivayam, K. Kadirvelu, Uptake of mercury(II) from wastewater by activated carbon from an unwanted agricultural solid by-product: Coirpith, *Carbon* 37 (1999) 79–84.
- [45] C. Namasivayam, K. Periasamy, Bicarbonate treated peanut hull carbon for mercury(II) removal from aqueous solution, *Water Res.* 27 (1993) 1163–1168.
- [46] M. Franz, H.A. Arafat, N.G. Pinto, Effect of chemical surface heterogeneity on the adsorption mechanism of dissolved aromatics on activated carbon, *Carbon* 38 (2000) 1807–1819.
- [47] B.K. Kim, S.K. Ryu, B.J. Kim, S.J. Park, Adsorption behavior of propylamine on activated carbon fiber surfaces as induced by oxygen functional complexes, *J. Colloid Interface Sci.* 302 (2006) 695–697.
- [48] M.J. Jung, E.Y. Jeong, J.W. Lim, S.I. Lee, Y.S. Lee, Physico-chemical surface modification of activated carbon by oxyfluorination and its electrochemical characterization, *Colloids Surf., A: Physicochem. Eng. Aspects* 389 (2011) 274–280.